JOURNAL OF MATERIALS SCIENCE: MATERIALS IN MEDICINE 9 (1998) 317–324

Isothermal and non-isothermal polymerization of a new bone cement

A. BORZACCHIELLO, L. AMBROSIO, L. NICOLAIS
Department of Materials and Production Engineering, University of Naples "Federico II" and Institute of Composite Materials Technology-CNR, P.le Tecchio 80, Naples, Italy

E. J. HARPER, K. E. TANNER, W. BONFIELD
IRC in Biomedical Materials, Queen Mary and Westfield College, University of London, Mile End Road, London E1 4NS, UK

A new bone cement based on poly(ethylmethacrylate) (PEMA), hydroxyapatite powder (HA) and *n*-butylmethacrylate monomer (*n*-BMA) has been studied using isothermal and non-isothermal polymerization. Methacrylate monomers are highly reactive and release a considerable amount of heat during polymerization. A quantitative understanding of the methacrylate polymerization is necessary because the thermal history of the polymerization has considerable influence on the final properties of a bone cement. In the first part, polymerization kinetics are analysed by means of differential scanning calorimetry (DSC). DSC data are used to evaluate a phenomenological model describing the cure kinetics of this new bone cement. In the second part, a kinetic model coupled with the energy balance is used to obtain temperature and degree of conversion profiles in the bone–cement–prosthesis system, under non-isothermal conditions, as function of initial temperature and thickness of the cement. Material properties, boundary and initial conditions and the kinetic behaviour are the input data for the numerically solved heat-transfer model. The temperature at the bone/cement interface, can be considered as a weak point, often responsible for total joint replacement failure. For this particular bone cement exhibiting a low exotherm and low glass transition temperature, the interfacial temperature is lower than the threshold level for thermal tissue damage (50 °C). The conversion occurs almost completely, avoiding problems with unreacted monomers that can be released by the cement, giving rise to tissue damage.

1. Introduction

Acrylic bone cements are widely used as a method of prosthetic component fixation in total hip-joint replacement surgery. Cements permit the immediate fixation of a prosthesis, but many short- and long-term effects are connected with their use. In PMMA bone cements, tissue necrosis may arise either from chemical or from thermal stimuli, giving rise to weakness of the cement/bone interface. This interface is considered to be a weak point often responsible for failure of the total joint replacement [1]. During the polymerization of methylmethacrylate, high peak temperatures are reached. Threshold levels for thermal tissue damage in bone are estimated to be between 48 and 60 °C. Within this temperature range, cell necrosis depends on the exposure time, which at 50 °C may be between 30 and 400 s. The temperature peak ranges from 48–105 °C at the bone/cement interface [2] and from 80–124 °C in the cement [3].

However, not only thermal effects are responsible for tissue necrosis [4]; in incomplete polymerization, a high level of unreacted monomer is slowly released by the cement, and may be responsible for tissue damage. For these reasons, the properties and performance of acrylic-based bone cements and the supporting bone are strongly dependent on their polymerization kinetics. Polymerization is a radical chain reaction: a radical reactive centre, once produced, adds many monomer units in a chain reaction and grows rapidly. At any instant, the reaction mixture only contains monomer, high molecular weight polymer and growing chains [5]. During polymerization, the rheological properties of the materials change substantially; the fluid bone cement transforms into a solid glass (vitrification).

Bulk polymerization of methacrylate is strongly influenced by diffusion at low and high values of the degree of conversion. At low conversion, the growth of high molecular weight molecules is responsible for a mobility reduction of the chain-end radicals, decreasing the possibility to form "dead polymers" and consequently increasing the rate of reaction ("gel effect" or "autoacceleration effect"). However, at high degrees of conversion, the glass transition temperature of the reaction mixture increases with the conversion of monomer to polymer and approaches the isothermal polymerization temperature (vitrification), strongly reducing the molecular mobility. Under these

0957–4530

conditions, the reaction becomes diffusion-controlled and the termination step of the polymerization is governed by this strong reduction in the molecular mobility determined by vitrification [6, 7]. The degree of conversion at the onset of the gel effect varies considerably, depending on the reaction conditions. A low-viscosity medium moderates the gel effect by increasing the degree of the conversion at which the gel effect begins. Alternatively, adding the polymer to the monomer, prior to initiating, increases the medium viscosity, shifting the gel effect towards a lower degree of conversion. In acrylic bone cements, a high fraction of polymeric filler is present, so the gel effect occurs at the beginning of the reaction, inducing a reduction of the reaction time and an accelerated reaction kinetic rate.

During setting of a bone cement in total hip replacement, the bone and the prosthesis take the roles of batch chemical reactor boundaries. A quantitative correlation between the temperature profiles and the degree of reaction across the bone–cement–prosthesis system, as a function of the process variables, is necessary because the final properties of the cement are highly influenced by the processing variables (mixing procedure, temperature and the geometry of the prosthesis and of the cavity). The only way to obtain a cement with repeatable properties is to control those variables fully [8].

In this paper, the isothermal and non-isothermal polymerization behaviour of a new bone cement, based on poly(ethylmethacrylate) (PEMA) powder and *n*-butylmethacrylate (*n*-BMA) developed at the IRC in Biomedical Materials is described [9, 10]. In the first part, the reaction kinetics are analysed by differential scanning calorimetry (DSC) and DSC data are used for the quantitative determination of the rates of polymerization in isothermal and non-isothermal conditions. The experimental data are used to evaluate the parameters of a phenomenological kinetic model. In the second part, the kinetic model is coupled with a heat-transfer model. The heat-transfer model is obtained by applying an energy balance across the prosthesis, bone and cement in order to predict the temperature in these parts and the degree of conversion in the cement as a function of the setting time, during non-isothermal polymerization. The full model is used to study the effects of different thicknesses and initial temperatures of the cement on the temperature and degree of reaction profiles across the bone–cement–prosthesis system. Material properties, boundary and initial conditions and the kinetic behaviour are the input data of the heat-transfer model that is solved numerically.

2. Materials and methods

2.1. Materials

The experimental IRC bone cement used in this investigation was based upon poly(ethylmethacrylate) powder (PEMA), containing 0.6 ($\pm$ 0.1) wt % residual benzoyl peroxide (BPO), (Bonar Polymers, Newton Aycliffe, Co. Durham, UK), hydroxyapatite (HA) powder (P81B HA powder supplied by Plasma Biotal Ltd, UK), and *n*-butylmethacrylate (*n*BMA) monomer stabilized with 0.01% quinol, including 2.5 vol %, *N*,*N*-dimethyl-*p*-toluidine (Aldrich Chemicals, UK). Extra BPO was added in the powder in the form of Lucidol CH50TM powder, consisting of 50 wt % BPO and 50 wt % di-cyclo-hexyl-phthalate (Peroxid-Chemie Ltd, Germany). The amount of HA powder, corresponding to a weight fraction of powder composition of 40%, was added in such a way to maintain the polymer to monomer weight ratio at 2:1. HA powder was added as reinforcement in an attempt to increase both the fatigue and the flexural properties of this new cement [9].

2.2. Methods

Differential scanning calorimetry is a widely used technique for studies of reaction kinetics [11–13]. A Perkin–Elmer DSC7, differential scanning calorimeter, was used. Dynamic scans at different heating rates (3, 5, 10 °C min^{-1}), from 0–180 °C, and isothermal measurements in the temperature range 10–35 °C, were carried out for 30 or 50 min. The sample weights ranged from 10–20 mg and the preparation was performed at 20 °C using a constant mixing time of 1 min. The overall time, from the contact of the monomer with the powder to the beginning of the DSC test, was 2 min. The samples, weighed after each experiment, showed negligible evaporation of monomer (less than 1%).

3. Results and discussion

3.1. Isothermal polymerization

Fig. 1 shows the thermogram of an isothermal test at 20 °C. An exothermic peak of reaction, after a time t_i, is present. This time is an important parameter from a processing point of view, because it is the only detectable macroscopic parameter representative of an initiator–inhibitor reaction [14]. The inhibitor (quinol) prevents incipient polymerization on storage and delays the onset of the polymerization reaction,

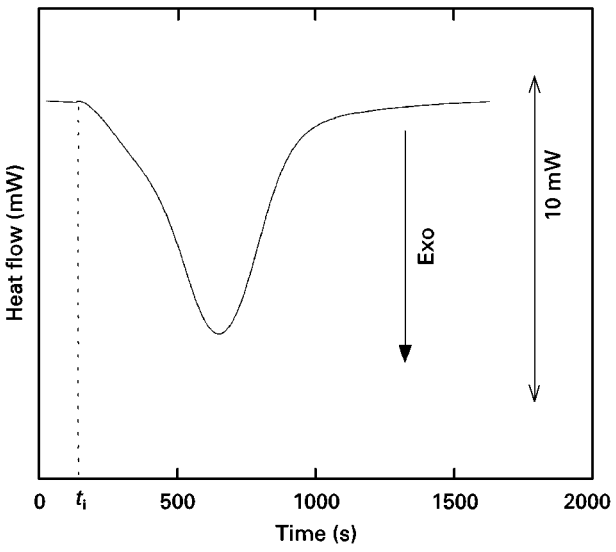

Figure 1 DSC thermogram obtained during isothermal polymerization at 20 °C.

which is essential during the operation for the insertion of the cement and positioning of the prosthesis. The time, t_i (induction time), shows the following temperature dependence, with the denominator a typical Arrhenius-type equation

$$t_i = 1/[K_{t0} \exp(-E_{t0}/RT)] \quad (1)$$

where K_{t0} is the pre-exponential factor, E_{t0} is the activation energy, R is the gas constant and T is the absolute temperature.

The induction time, obtained from DSC tests, was corrected for the sample preparation time. At 20 °C, the handling time and the induction time, measured from the DSC, were summed to obtain the true t_i; the ratio between the handling time and the true induction time at 20 °C was used to correct the induction time observed at the other temperatures. The corrected induction times were used to compute the parameters of Equation 1 by linear regression (Table I). A good agreement between experimental data and model results is observed in Fig. 2.

DSC measurements are also useful as they enable the determination of the degree of polymerization. It may be assumed that the heat evolved during the polymerization reaction is proportional to the overall extent of reaction given by the fraction of reactive groups consumed. Using this approach, the degree of reaction, α, is defined as

$$\alpha = H(t)/H_{tot} \quad (2)$$

where $H(t)$ is the heat developed in a DSC experiment between the starting point and a given time, t; and H_{tot} represents the total heat developed. Total heat is calculated by integrating the total area under the DSC curve in a non-isothermal experiment. The reaction rate, $d\alpha/dt$, is thus obtained from the heat flow, dH/dt, as

$$\frac{d\alpha}{dt} = \frac{1}{H_{tot}} \frac{dH}{dt} \quad (3)$$

For the IRC bone cement, a value of 100 J g^{-1} was obtained for H_{tot}, by averaging the reaction heats measured in non-isothermal experiments. The total heat for this bone cement based on *n*BMA monomer is lower than that for PMMA cement, and the polymerization heats of MMA and BMA are 576 and 418 J g^{-1}, respectively [15].

Isothermal DSC experiments show that the developed heat, H_{is}, is lower than H_{tot}, thus indicating the presence of unreacted monomer. This may be revealed by heating a sample immediately after an isothermal polymerization (Fig. 3). Curve (a) is the thermogram obtained by heating, at 10 °C min^{-1}, of a sample previously polymerized at 20 °C. In this thermogram, a residual reactivity peak is present, indicating that the material is not fully polymerized. This peak is shifted to a higher temperature than the test temperature because vitrification is unable instantaneously to arrest the reaction, as has been observed for thermosetting resins [14, 16, 17]. This shift may result in the glass transition temperature, T_g, reaching a higher temperature than the polymerization temperature. A maximum degree of conversion, α_{max}, may be introduced

$$\alpha_{max} = \frac{H_{is}}{H_{tot}} \quad (4)$$

It was found that α_{max} increases with increasing isothermal polymerization temperature according a linear law. Fig. 4 shows that a linear regression [16, 17]

$$\alpha_{max} = p + qT \qquad \text{for } T < T_{g,max} \quad (5)$$

is a good representation of DSC experimental data.

TABLE I Parameters of the full kinetic model

Parameter	Value
n	1.14
m	0.98
$\mathrm{Ln}(K_0)$ (s^{-1})	9.4
E_a/R (K)	4000
p	− 1.584
q (K^{-1})	0.008
$\mathrm{Ln}(K_{t0})$ (s^{-1})	− 24.5
E_{t0}/R (K)	9000

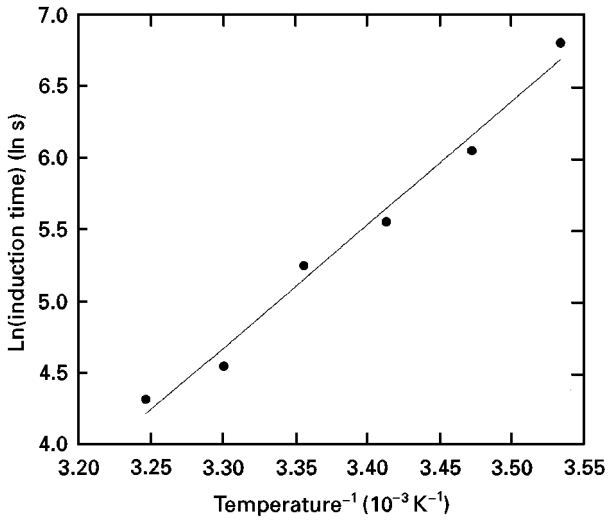

Figure 2 Isothermal induction time as function of temperature.

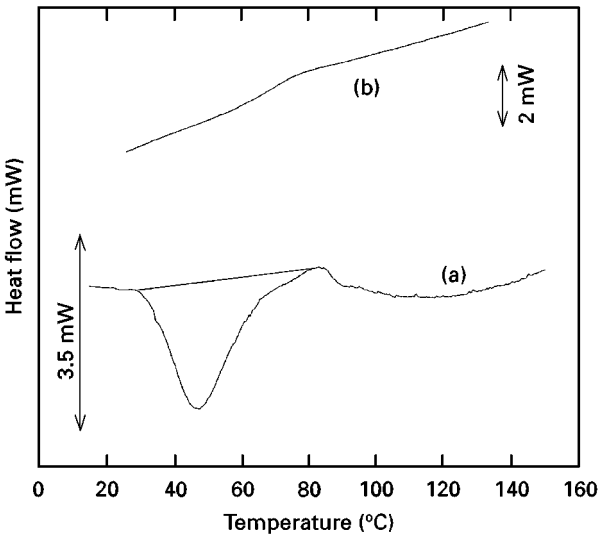

Figure 3 DSC thermograms obtained by heating at 10 °C min^{-1} for (a) sample cured at 20 °C and (b) fully cured sample.

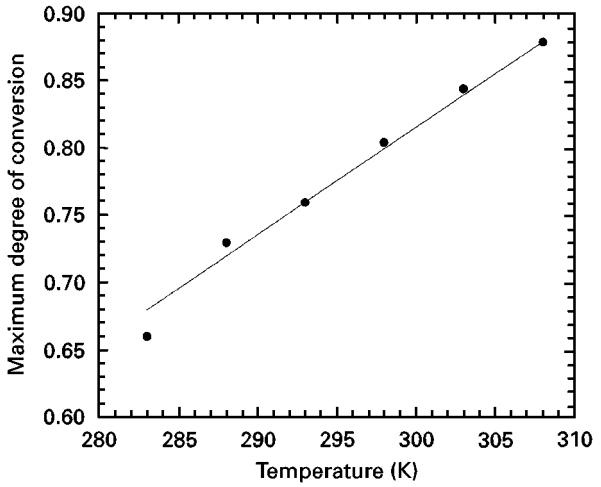

Figure 4 Maximum degree of conversion obtained in isothermal DSC polymerization experiments as function of temperature.

The fitting parameters p and q are reported in Table I. A dynamic DSC scan of a sample previously subjected to a dynamic DSC scan does not show a residual peak (Fig. 3, curve (b)), indicating that the sample is fully polymerized. When the scan temperature approaches the glass transition temperature of the fully polymerized system, $T_{g\max}$, α_{max} goes to 1. The thermogram, in curve (b), shows a glass transition temperature of approximately 70 °C for the IRC bone cement. This transition temperature is considerably lower than that of PMMA (105–113 °C) [18]. The new IRC cement is a partially inter-penetrating network system based on ethylmethacrylate and butylmethacrylate polymers with T_gs of 65 and 32 °C, respectively [10].

The chain polymerization reaction, as mentioned above, is dominated by the diffusion effect at the beginning (gel effect) and at the end of polymerization (vitrification). In particular, the gel effect is shifted at the beginning of the reaction because of the high fraction of inert polymer added to the monomer [19].

Many complex models have been reported in the literature for the polymerization of methacrylate [19–21]. However, as the onset of the gel effect is shifted at the start of the reaction, it is possible to use a simplified kinetic model. A simple pseudo-autocatalytic expression, previously proposed for polyester and acrylic thermosetting resins, may be used [14, 22]

$$\frac{d\alpha}{dt} = K(\alpha_{max} - \alpha)^n \alpha^m \quad (6)$$

where m and n are non-temperature-dependent fitting parameters and K is a temperature-dependent rate constant given by an Arrhenius-type equation

$$K = K_0 \exp\left(\frac{-E_a}{RT}\right) \quad (7)$$

where K_O is the pre-exponential factor, R is the gas constant, E_a is the activation energy, and T is the absolute temperature. The temperature dependence of α_{max} in Equation 6 is given by Equation 5.

The theoretical model given by Equations 1, 5–7 correlates well with the experimental degree of reaction and the rate of reaction obtained by DSC tests at between 20 and 35 °C, the temperatures investigated. This is clearly shown in Fig. 5 of a DSC performed at 20 °C. As the temperature increased, the rate of reaction increased, giving a higher peak which occurred earlier and the degree of conversion increased reaching 0.88 at 35 °C. Furthermore, the model predicts the transition to a glassy state, with the rate of reaction during an isothermal polymerization approaching zero as α tends to α_{max}.

The values of the kinetic parameters of the model, evaluated by regression analysis, are listed in Table I.

3.2. Non-isothermal polymerization

In a bone–cement system, non-isothermal conditions occur because of the high exothermic nature of the reaction. For thick cement layers, not all the heat generated is dissipated sufficiently quickly to maintain isothermal conditions. The kinetic model used closely predicts the non-isothermal polymerization. Fig. 6

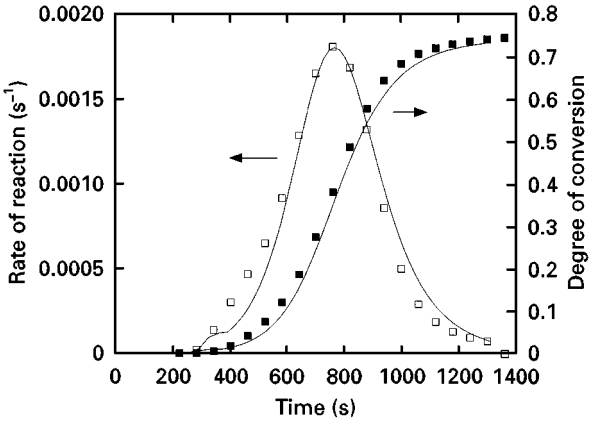

Figure 5 Comparison between kinetic model predictions and (○) experimental degree of conversion and (●) experimental rate of reaction at 20 °C.

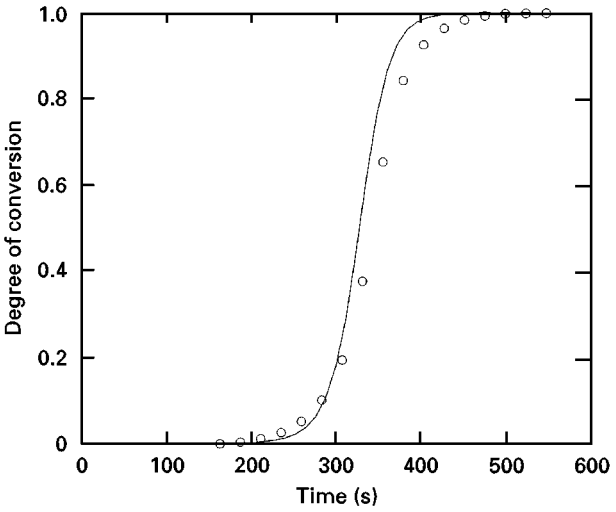

Figure 6 Comparison between kinetic model predictions and (○) experimental degree of conversion in non-isothermal conditions (heating rate 10 °C min^{-1}).

shows the comparison between the degree of conversion obtained by a dynamic DSC test and the model predicting degree of conversion. In non-isothermal conditions, the induction time, t_{ni}, may be calculated as the sum of the contributions at each isothermal temperature step

$$Q = \int_0^{t_{ni}} \frac{dt}{t_i} \tag{8}$$

where t_i is the isothermal induction time given by Equation 1 and Q is a dimensionless parameter ranging from 0–1. The time at which Q is equal to 1, represents the non-isothermal induction time.

In order to predict the temperature profiles across the bone, the cement and the prosthesis, and the degree of conversion in the cement as function of the setting time during the non-isothermal polymerization, the appropriate kinetic model must be coupled with the energy balance, that allows material thicknesses, the initial temperature differences between the components and the ability of different materials to dissipate heat, to be included.

The following assumptions are used.

1. Heat is dissipated in the radial direction (r-axis) only, according to the axial section sketched in Fig. 7.
2. The values of density, ρ, specific heat, C_p, and thermal conductivity, k_r, for the bone are given as $1.7\,g\,cm^{-3}$, $1.25\,J\,g^{-1}\,K^{-1}$, $0.43\,W\,m^{-1}K^{-1}$, respectively [23], and for the steel prosthesis $7.8\,g\,cm^{-3}$, $0.5\,J\,g^{-1}\,K^{-1}$, $10.3\,W\,m^{-1}\,K^{-1}$, respectively [24]. For the cement the density is calculated as a weighted average of the densities of PEMA ($1.119\,g\,cm^{-3}$), PBMA ($1.055\,g\,cm^{-3}$) [25] and HA density ($3.156\,g\,cm^{-3}$) [26]. The specific heat was calculated from DSC experiments ($2\,J\,g^{-1}\,K^{-1}$). The thermal conductivity was calculated as a weighted average of k_r for HA ($1.3\,W\,m^{-1}\,K^{-1}$) and PMMA ($0.17\,W\,m^{-1}\,K^{-1}$) which is close to value of k_r for PEMA and PBMA.

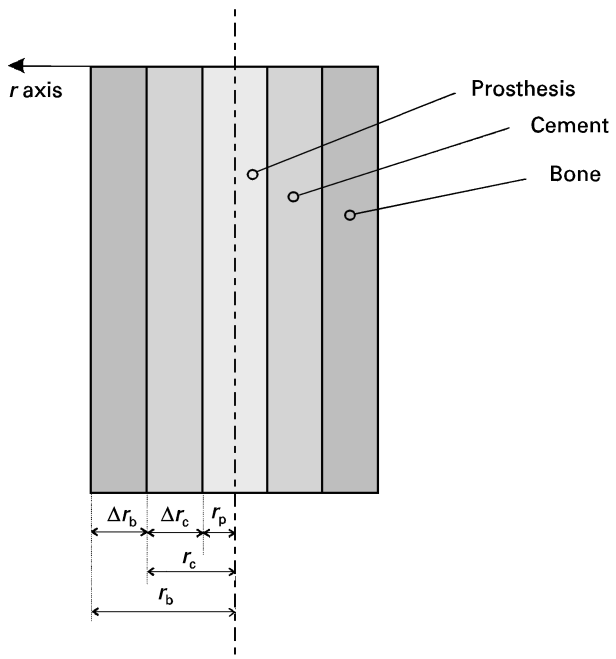

Figure 7 Sketch of the geometry used for the polymerization simulation.

Using the assumptions, the law of conservation of energy in the bone and the prosthesis takes the form

$$\rho_i c_{pi} \partial T/\partial t = k_{ri}(\partial^2 T/\partial r^2 + 1/r\ \partial T/\partial r) \qquad i = b, p \tag{9}$$

where b and p indicate the properties of bone and prosthesis, respectively. In the cement, the energy balance then becomes

$$\rho_i c_{pi}\, \partial T/\partial t = k_{ri}(\partial^2 T/\partial r^2 + 1/r\ \partial T/\partial r) + \rho_c\, dH/dt \tag{10}$$

where (dH/dt) is the rate of heat generated by chemical reaction. dH/dt is given by Equation 3, in which the rate of reaction $d\alpha/dt$ is calculated from the kinetic model (Equations 5–7).

To facilitate the numerical solution of Equations 9 and 10, the following dimensionless variables are introduced:

dimensionless temperature

$$\theta = (T - T_0)/(T_{ref} T_0) \tag{11a}$$

dimensionless time

$$t^* = t/t_{1/2} \tag{11b}$$

dimensionless position

$$r^* = r/\Delta r_i \qquad i = p, c, b \tag{11c}$$

where Δr_i represents the prosthesis radius, the thickness of the cement or the bone (Fig. 7), T_0 is the initial temperature of the cement, T_{ref}, 37 °C, is taken as the reference temperature and $t_{1/2}$ is defined as the time needed to reach a value of $\alpha = 0.5$. $t_{1/2}$ is obtained by numerical integration, at $T = T_{ref}$, of the kinetic model given by Equations 5–7.

Substituting the dimensionless variables given by Equations 11 in Equations 9 and 10, respectively, the energy balance for the bone and the prosthesis then becomes

$$\partial\theta/\partial t = De_i(\partial^2\theta/\partial r^{*2} + 1/r^*\,\partial\theta/\partial r^*) \qquad i = b, p \tag{12}$$

and for the cement

$$\partial\theta/\partial t = De_c(\partial^2\theta/\partial r^{*2} + 1/r^*\,\partial\theta/\partial r^*) + St\, d\alpha/dt^* \tag{13}$$

$$d\alpha/dt^* = K^* \exp(-E_a/RT)\alpha^m(\alpha_m - \alpha)^n \tag{14}$$

Equation 14 is the dimensionless form of the kinetic model (Equation 6) where K^* is a dimensionless kinetic constant, given by

$$K^* = t_{1/2} K_0 \tag{15}$$

In Equations 12 and 13, De_i is the dimensionless diffusion Deborah number, given by

$$De_i = \frac{k_{ri} t_{1/2}}{\rho_i C_{p_i} (\Delta r_i)^2} \tag{16}$$

The Deborah number represents the relative importance of the heat transferred by conduction with

respect to the heat accumulated in the material. In Equation 13, the dimensionless group

$$\mathrm{St} = \frac{Q_{\mathrm{tot}}}{(T_{\mathrm{ref}} - T_0)C_{\mathrm{p_c}}} \tag{17}$$

is the Stefan number, expressing the relative weight of the latent heat associated with the chemical reaction with respect to the accumulation of heat in the material. In terms of these dimensionless groups, isothermal polymerization conditions are obtained if $\mathrm{De} \gg \mathrm{St}$. This implies that in the energy balance, the contribution of the thermal diffusivity (Deborah number) is much higher than the contribution of heat generation due to the polymerization reaction (the Stefan number). The Deborah numbers of the bone and prosthesis are a measure of their ability to dissipate the heat generated in the cement by polymerization. The Deborah number is affected by its thickness, in addition to the material properties (ρ, C_{p}, and k_{r}).

In Equations 12–14, with these assumptions, the initial conditions are

$$\begin{array}{ll} \text{Prosthesis} & t^* = 0 \;\; \theta = \theta_{\mathrm{p0}} \\ \text{Cement} & t^* = 0 \;\; \theta = \theta_{\mathrm{c0}} \;\; \alpha = 0 \\ \text{Bone} & t^* = 0 \;\; \theta = 1 \end{array} \tag{18}$$

where θ_{p0} and θ_{c0} are given by Equation 11a–c, calculated at the initial temperature of prosthesis and cement, respectively. The dimensionless boundary conditions are

Prosthesis:

$$\begin{array}{ll} r^* = 0 & (\partial\theta/\partial r^*) = 0 \\ r^* = 1 & (\partial\theta/\partial r^*)_{\mathrm{rp}} = K^*_{\mathrm{rpc}}(\partial\theta/\partial r^*)_{\mathrm{rc}} \quad \theta_{\mathrm{p}}(1) = \theta_{\mathrm{c}}(0) \end{array} \tag{19a}$$

Cement:

$$\begin{array}{ll} r^* = 0 & (\partial\theta/\partial r^*)_{\mathrm{rp}} = K^*_{\mathrm{rpc}}(\partial\theta/\partial r^*)_{\mathrm{rc}} \quad \theta_{\mathrm{p}}(1) = \theta_{\mathrm{c}}(0) \\ r^* = 1 & (\partial\theta/\partial r^*)_{\mathrm{rc}} = K^*_{\mathrm{rcb}}(\partial\theta/\partial r^*)_{\mathrm{rb}} \quad \theta_{\mathrm{c}}(1) = \theta_{\mathrm{b}}(0) \end{array} \tag{19b}$$

Bone:

$$\begin{array}{ll} r^* = 0 & (\partial\theta/\partial r^*)_{\mathrm{rc}} = K^*_{\mathrm{rcb}}(\partial\theta/\partial r^*)_{\mathrm{rb}} \quad \theta_{\mathrm{c}}(1) = \theta_{\mathrm{b}}(0) \\ r^* = 1 & \theta = 1 \end{array} \tag{19c}$$

The equality of the heat flow and of the temperatures at the prosthesis/cement and cement/bone interfaces is imposed by means of Equations 19a–c. The dimensionless groups Kr_{pc} and Kr_{cb} are defined as

$$Kr_{\mathrm{pc}} = \frac{kc_{\mathrm{rp}}}{kp_{\mathrm{rc}}} \tag{20}$$

$$Kr_{\mathrm{cb}} = \frac{kb_{\mathrm{rc}}}{kc_{\mathrm{rb}}} \tag{21}$$

A numerical solution of the mathematical model presented, Equations 14–16, is performed using implicit finite differences.

3.2.1. Model results and discussion

The polymerization process is simulated referring to the geometry sketched in Fig. 7. The effect of the cement thickness and of the insertion temperature are considered in the proposed case studies. Two different initial temperatures are considered: 5 °C (pre-cooled cement) and 18 °C (ordinary room temperature). Each case is considered with three different cement thicknesses: 3, 5 and 8 mm. The thickness of the elements and the initial and boundary conditions used are summarized in Tables II and III.

For simulation 5 (Table II), a preparation time of 2.5 min at 5 °C was assumed. For simulations 18, a preparation time of 2.5 min at 18 °C was assumed. Figs 8 and 9 show the profiles of temperature and degree of conversion, respectively, as function of polymerization time at the bone/cement interface for the three different thicknesses of simulation 18. During the polymerization, the temperature is always lower than 50 °C, reaching a maximum of 49 °C for the thickest layer. The degree of conversion is higher than 90% for all three cement thicknesses. The thicker the cement layer the higher are both the maximum temperature and the degree of conversion. Pre-cooling the cement to 5 °C (simulation 5) results in a temperature below 48 °C and a degree of conversion greater than

TABLE II Dimensions of prosthesis, bone and cement used for the simulations

Simulation	Prosthesis radius (mm)	Cement thickness (mm)	Bone thickness (mm)
S5, S18	10	3	8
M5, M18	10	5	8
L5, L18	10	7	8

TABLE III Initial conditions used for the simulations

Simulation	Prosthesis temp. (°C)	Cement temp. (°C)	Bone temp. (°C)
S5, M5, L5	18	5	37
S18, M18, L18	18	18	37

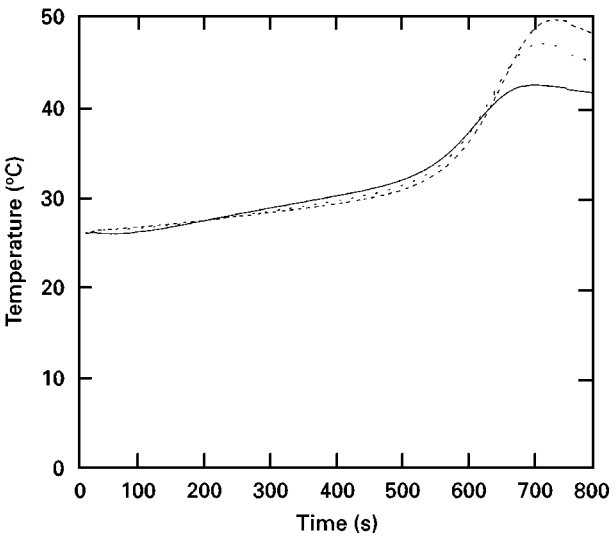

Figure 8 Results of the numerical simulation: polymerization time dependence of temperature at the bone/cement interface for three different thicknesses (simulations S18, M18, L18). (—) 3 mm, (- - -) 5 mm, (– – –) 7 mm.

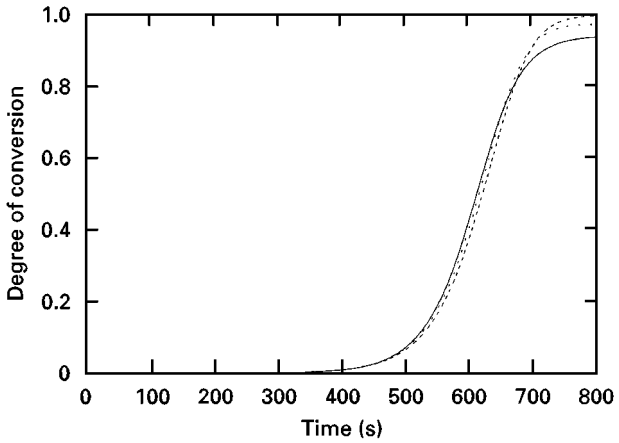

Figure 9 Results of the numerical simulation: polymerization time dependence of degree of conversion at the bone/cement interface for three different thicknesses (simulations S18, M18, L18). (—) 3 mm, (- - -) 5 mm, (– – –) 7 mm.

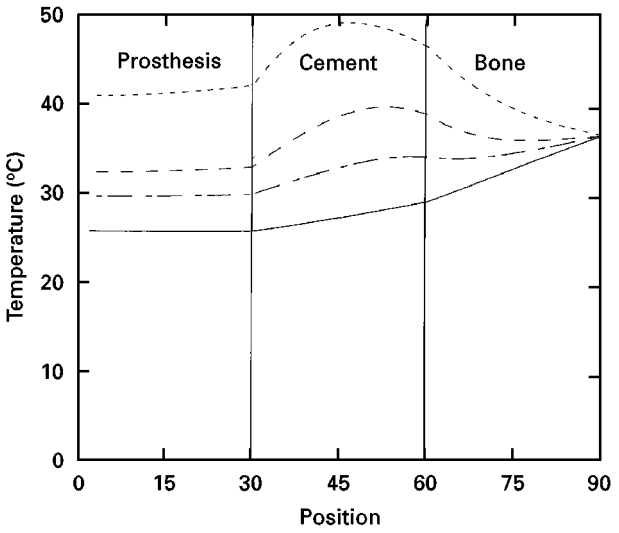

Figure 10 Results of the numerical simulation: temperature profile across the system for simulation M18 at different times. (—) 365 s, (- – -) 567 s, (– – –) 618 s, (- - -) 689 s.

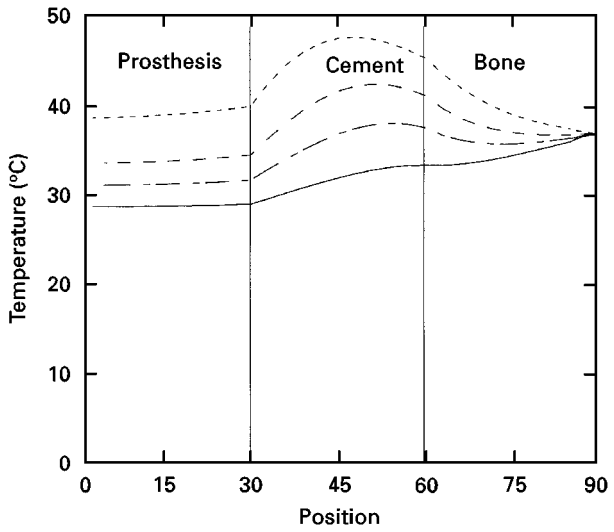

Figure 11 Results of the numerical simulation: temperature profile across the system for simulation M5 at different times. (—) 699 s, (- – -) 750 s, (– – –) 780 s, (- - -) 820 s.

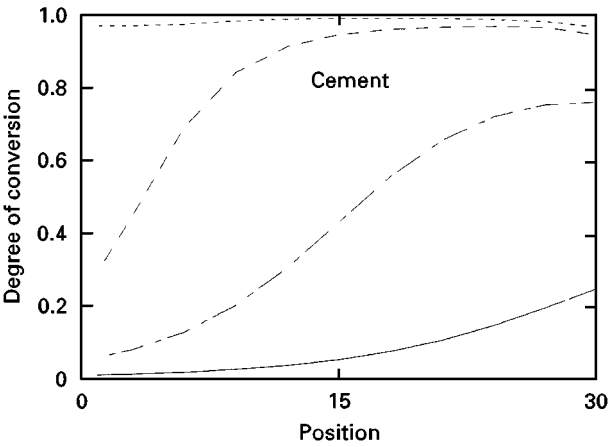

Figure 12 Results of the numerical simulation: conversion profile across the cement for simulation M18 at different times. (—) 425 s, (- – -) 517 s, (– – –) 588 s, (- - -) 851 s.

90%. The pre-cooling process slows the polymerization as it is completed in 1000 s compared to the 800 s necessary to complete the polymerization in the case of a starting temperature of 18 °C. The higher the starting temperature, the higher the maximum temperature reached and the greater the degree of conversion. However, even with the highest starting temperature and thickest cement layer, the maximum temperature was below 50 °C and with the lowest starting temperature and thinnest cement layer the degree of conversion was about 90%.

Figs 10 and 11 show temperature profiles across the prosthesis, cement and bone, for simulations 5M and 18M, respectively, and are reported after varying times. The peak temperature, started at the cement/bone interface and moved into the middle of the cement. The temperature profiles clearly show that adiabatic polymerization occurred for a cement thickness of 5 mm, but analogous profiles were obtained for the thinner and the thicker layers. For the PEMA cement the Stefan number has a value of 2.6 and a Deborah number an order of magnitude higher obtained for a cement layer of 1.4 mm, thinner than commonly used clinically. For the PEMA cement, even in the middle of the thickest layer, which is the highest temperature reached, the temperature is below 60 °C. Fig. 12 shows the uniformity of the degree of conversion throughout the cement thickness at the end of polymerization (simulation M18).

4. Conclusions

The isothermal and non-isothermal polymerization of a new bone cement has been studied. A simple phenomenological model was successfully used to describe the polymerization reaction of cement. This model was integrated with an energy balance to predict temperature and degree of conversion across the bone–cement–prosthesis system. The characteristics of the PEMA cement (low exotherm and low glass transition temperature) resulted in the temperature at the bone/cement interface being less than 50 °C and

gave a conversion higher than 90%. Therefore, this simulation shows that the application of this cement will not result in problems of tissue necrosis from either thermal or chemical stimuli.

References

1. P. C. NOBLE, *Biomaterials* **4** (1983) 94.
2. G. M. BRAUER, D. R. STEINBERGER and J. W. STANSBURY, *J. Biomed. Mater. Res.* **20** (1986) 839.
3. S. SAHA and S. PAL, *ibid.* **18** (1984) 435.
4. C. D. JEFFERISS, A. J. C. LEE and R. S. M. LING, *J. Bone Jt Surg.* **57 B** (1975) 511.
5. G. ODIAN, "Principles of polymerization" (McGraw-Hill, New York, 1988).
6. I. MITA, K. HORIE, *JMS-Rev. Macromol. Chem. Phys.* C 27 (1) (1987) 91.
7. A. MAFFEZZOLI, R. TERZI and L. NICOLAIS, *J. Mater. Sci. Mater. Med.* **6** (1995) 155.
8. L. W. SWENSON, D. J. SCHURMAN and R. L. PIZIALI, *J. Biomed. Mater. Res.* **15** (1981) 83.
9. E. J. HARPER, J. C. BEHIRI and W. BONFIELD, *J. Mater. Sci. Mater. Med.* **6** (1995) 799.
10. R. L. CLARKE and M. BRADEN, *J. Dental Res.* **61** (1982) 997.
11. L. MIGLIARESI, L. FAMBRI and J. KOLARIK, *Biomaterials* **15** (1994) 875.
12. J. A. FELIU, C. SOTTILE, C. BASSANI, J. LIGTHART and G. MASCHIO, *Chem. Eng. Sci.* **51** (1996) 2793.
13. J. M. YANG, J. W. YOU, H. L. CHEN and C. H. SHIH, *J. Biomed. Mater. Res.* **33** (1996) 83.
14. J. M. KENNY, A. MAFFEZZOLI and L. NICOLAIS, *Compos. Sci. Technol.* **38** (1990) 339.
15. F. MARK, "Encyclopedia of Chemical Technology", Vol. 15, 3rd Edn, (Wiley, New York, 1981).
16. J. M. KENNY and A. TRIVISANO, *Polym. Eng. Sci.* **31** (1991) 1426.
17. A. MAFFEZZOLI, A. DELLA PIETRA, S. RENGO, L. NICOLAIS and G. VALLETTA, *Biomaterials* **15** (1994) 1221.
18. J. BRANDRUP and E. H. IMMERGUT, "Polymer Handbook" (Wiley Interscience, 1989).
19. K. A. HIGH, H. B. LEE and D. T. TURNER, *Macromolecules* **12** (1979) 332.
20. J. M. DIONISIO and K. F. O'DRISCOLL, *J. Polym. Sci. Polym. Chem.* **18** (1980) 241.
21. R. SACK, G. V. SCHULZ and G. MEYERHOFF, *Macromolecules* **21** (1988) 3345.
22. A. MAFFEZZOLI, R. TERZI and L. NICOLAIS, *J. Mater. Sci. Mater. Med.* **6** (1995) 161.
23. B. N. FEINBERG, "Handbook of Engineering in Medicine and Biology" (CRC Press, Cleveland, 1978).
24. F. KREITH, "Principles of Heat Transfer" (Dun-Donnelley, New York, 1973).
25. T. KIJIMA and M. TSUTSUMI, *J. Am. Ceram. Soc.* **62** (1979) 9.
26. S. SAHA and S. PAL, *J. Biomed. Mater. Res.* **18** (1984) 435.

Received 24 June
and accepted 1 September 1997